A Widely-Tunable RF Receiver Employing Synthetic Diversity for Interference Mitigation

Sanaz Sadeghi, Sweta Soni and Alyosha Molnar
Department of Electrical and Computer Engineering, Cornell University, Ithaca, NY, USA
Email: {ss3842,ss3964,am699}@cornell.edu

2022 IEEE International Symposium on Circuits and Systems (ISCAS) | 978-1-6654-8485-5/22/$31.00 ©2022 IEEE | DOI: 10.1109/ISCAS48785.2022.9937610

***Abstract*—This paper presents a novel technique for suppression of in-band artifacts from out-of-band (OOB) interference in widely tunable RF receivers. The technique employs a multi-tap inductor-capacitor network (LCN) to generate diversity in gain and phase between taps across the targeted frequency range. Using this network to feed a bank of identical receivers sharing a single local oscillator (LO) allows multiple kinds of interferer artifact to be suppressed. Here we considered spur-induced and phase noise-induced artifacts. In each case, the resulting artifacts are linearly separable from signal when the outputs of the sub-receivers are recombined. AC and transient simulations were first performed to show feasibility of the proposed approach. A prototype was implemented in 45nm CMOS which confirmed the validity of the synthetic diversity (SD) approach for suppressing interferer artifacts, showing a maximum lowering in EVM and BER of 38% and 60% respectively.**

Keywords—Out-of-band interferer, phase noise, interferer suppression, front-end

I. INTRODUCTION

With increasing dynamic occupancy of the RF spectrum, it is desirable that RF receivers be able to tune across an octave or more of center frequency in order to avoid strong interferers, and make opportunistic use of unoccupied spectrum. At the same time, the increased numbers of users requires such a receiver to also withstand strong interferers at other frequencies in the desired frequency range.

Tunable oscillators combined with frequency dividers can be used to realize multi-octave frequency tuning (albeit at a cost in phase noise (PN) and power consumption), and if a wide-band antenna is used, good sensitivity can be achieved across similarly wide tuning range using wide-band LNAs and mixers ([1], [2]). The big challenge for tunable radios is in their resilience to interference, since wide tuning tends to disallow the use of highly selective band-pass filters.

Receiver sensitivity is degraded in the presence of strong OOB interference by non-idealities in the receiver itself. Specifically, nonlinearity, as well as spectral impurities in the receiver's LO, such as spurs and PN, can interact with strong OOB interferes to generate in-band artifacts (IBAs) that are indistinguishable from, and so corrupt the desired in-band signal. Circuit techniques such as harmonic rejection, N-path filtering and passive mixer-first architectures have helped to alleviate the OOB interferer issue, especially with respect to nonlinearity, ([3]-[6]), but still need a very clean LO to avoid reciprocal mixing of phase noise or spurious tones. In this paper we explore an alternate receiver architecture, based on the concept introduced in [7], with a wide tuning range and enhanced OOB interference tolerance even in the context of a receiver with a high PN LO.

This work was supported in part by NSF Grant #2030207 and was supported in part by the Semiconductor Research Corporation (SRC) and DARPA, and was performed in part at the Cornell NanoScale Facility, an NNCI member supported by NSF Grant NNCI-2025233.

II. CONCEPT AND THEORY

As depicted in Fig. 1, spectral impurities in the LO, like PN and spurs, get mixed with strong interference and fall in band, raising the noise floor and burying weak wanted signals beyond recovery.

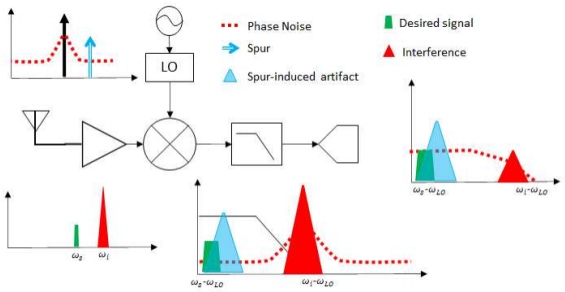

Figure 1. In-band artifacts from OOB interference. The input has wanted signal and the interference. Non-idealities of the LO interact with OOB interference to generate IBAs.

Synthetic diversity (SD), as introduced in [7], creates channel diversity akin to that in multi-input multi-output (MIMO) systems. Here, diversity comes from an LCN at the input, which splits the signal from a single antenna to N sub-receivers. The LCN acts to apply complex gains to the N outputs, with the resulting gain vector depending strongly on frequency. The signal and OOB interferer see different complex gain vectors (CGVs) which the IBAs inherit, so that when the N outputs are recombined in the digital domain, the wanted signal can be recovered while IBAs are cancelled. Since the N outputs are combined coherently at the output, each sub-receiver can be N times noisier (and so lower power) without significantly degrading overall noise performance [7].

The LCN interacts with a signal at frequency , and interferer, at frequency , by applying complex gains vectors () and (). Entries in () represent the transfer function of the LCN from input to each of the N outputs. In [7], it was shown that the signal becomes a vector
() and IBAs inherit weights from the OOB interferers that create them: 1) PN reciprocal mixing appears as = (−)(), where (−) is PN of the LO at the and 2) spur, at frequency , mixing appears as
= ().

IBAs inherit different CGVs from the signal, and if these CGVs are sufficiently incoherent to the signal CGV, one can weight and recombine the N outputs to cancel the artifact and preserve the signal, as illustrated in Fig. 2.

III. SYSTEM SIMULATIONS

To validate the SD concept, we performed frequency- and time-domain simulations in MATLAB, incorporating non-

idealities of the LO and compared performance with and without the SD LCN. We modelled the input with both the QPSK signal and OOB interferer, where the interferer strength was 300 times stronger than the signal, and swept the frequency of the interferer (F_{int}) from 1GHz to 2GHz with the signal frequency (F_{sig}) at 1.5GHz. An example LCN used for performing time domain simulations is shown in Fig. 2. The design approach for these networks will be discussed in section IV.

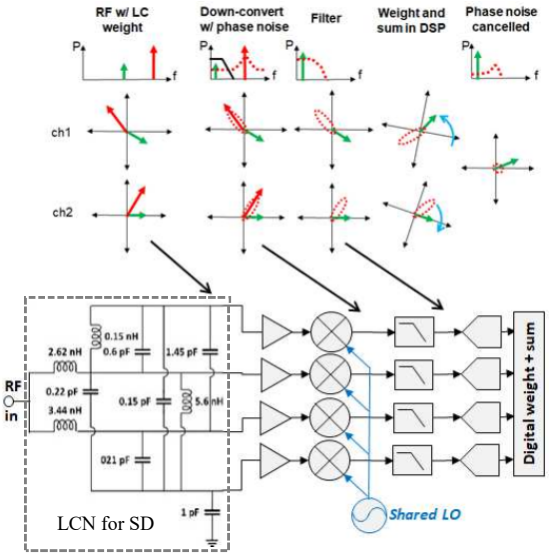

Figure 2. SD Concept: Diversity between interference (red) and signal (green) is preserved throughout the receive chain. While the OOB interfere (red arrow) is suppressed by low pass filtering, PN artifacts survive, (dashed oval) but is suppressed after complex weighting and summing [7].

After passing the input through the diversity networks it is fed into a model of LNA, mixer and baseband filtering, incorporating LNA noise, and LO PN or spurs. The baseband outputs are then complex weighted and combined. Based on the CGVs of signal and IBA, recombining weights, , were found to minimize the IBA component and maximize the signal component, following the approach outlined in [7]. Specifically, is chosen so that the projection of the output onto () is maximized while the projection onto the artifacts, , is minimized. is a function of interferer CGV, () (Fig. 2). For an optimized SNR, weights need to be set as = () – [7]. As described in [7]. These weights can be found using a blind algorithm without *a-priori* knowledge of the interferer's frequency.

In fact, since multiple interference mechanisms can act at once, ( ) may cover a subspace of dimensions greater than one. We, therefore, used principal component analysis (PCA) on the interference to find . Presence of more than one IBA, more than one principal component (PC) is expected to be strong enough to need to be suppressed.

We modelled two types of LO impurity: a spurious tone at the interferer frequency, and phase noise. These impurities reciprocally mix with a QPSK modulated OOB interferer to generate IBA. Fig. 3(a) shows the output in the presence of a spur in the LO spectrum that lines up with the interferer's frequency, causing the interference to mix into our signal band and corrupt the signal (red data points). The blue points represent the output after passing through the SD network and summing with proper weights as described above. SD results in a cleaner constellation and a significant improvement in EVM as shown in Fig. 3(b). Similarly, we modelled the PN which resulted in the constellation shown in Fig. 3(c). Once again, we compared the output of a simple receiver (red points) to the recombined output of a receiver with SD LCN. EVM across frequency is shown in Fig. 3(d). Note that we included some low-Q filtering on the PN, with a 3-dB bandwidth of 200MHz since strong white noise in the LO that reaches the 3rd harmonic of the LO can cause additional mixing terms ([7], [8]).

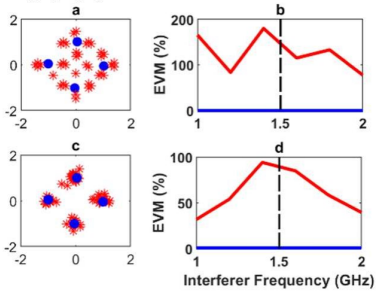

Figure 3. Effect of different types of artifacts on output constellations and comparison with the suppressed version. F_{sig} is 1.5GHz for all cases. Shown constellations are for F_{int} of 1.6 GHz. a and b show simulation results for spur, c and d for PN. Dashed lines show LO frequency.

IV. DIVERSITY NETWORK DESIGN

The function of the LC SD network is to generate transfer functions that minimize the inner product () · ()* for any choice of and in the receiver's frequency tuning range, while simultaneously minimizing the loss in signal power (summed across the N outputs) to ensure a good NF for any signal in the receiver's frequency range. These requirements do not, however, reveal what LCN topology is optimal for achieving these goals.

One potential network we explored was a bank of LC bandpass filters, each having a slightly different resonant frequency to achieve diverse gain and phase responses across different frequencies, as shown in Fig 4. Using this network, transient simulations were performed for a F_{sig}=1.5 GHz to assess interferer suppression. Fig. 5(a) and Fig. 5(b) show the results of transient simulations. As shown here, the designed LC network provides enough diversity to recover signals that otherwise are completely submerged in IBAs. However, for some cases, e.g. F_{int}=1GHz here, the network is less effective.

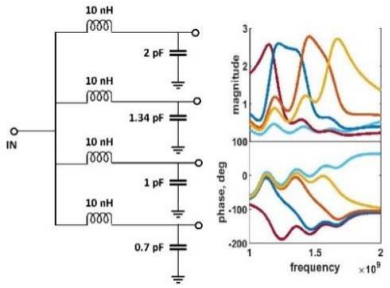

Figure 4. Designed bank of band pass filter as frontend diversity network

To better explore what constitutes an "optimal" LCN, we employed an optimization algorithm (similar to that in [7]) to search for a network that minimizes the weighted sum of: 1) average NF across the frequency band of interest, in the absence of interference 2) NF after cancellation of IBAs,

averaged across all combinations of interferer and signal frequency in the band of interest, and 3) a cost related to the number and value of the L's and C's in the network. This optimization was fed an initial topology and employed a mix of gradient descent and random permutation. Fig. 6 shows an example of such optimized network using the network in Fig. 4 as a starting point. The result does not resemble a known structure and looks almost random.

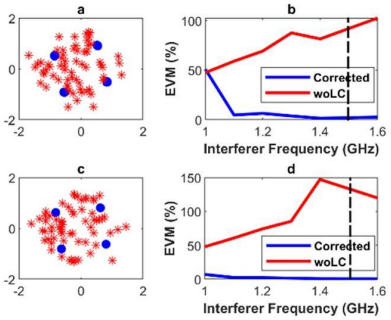

Figure 5: Comparison of designed vs optimized network, for F_{sig}=1.5GHz. a) Constellation of the designed network for F_{int}=1.6GHz, b) EVM vs Interferer frequency for designed network, c) Constellation of optimized network for F_{int}=1.6GHz, d) EVM vs Interferer frequency for optimized network. Dashed lines show LO.

To test whether the algorithm effectively optimizes the network for interferer suppression, we performed the same transient simulations as in Fig. 5 (a), (b) for the network of Fig. 6, with the result presented in Fig. 5 (c), (d). As seen here, the constellations are cleaner and suppression is successfully performed for all cases. Interestingly, because the optimization algorithm is stochastic, re-running the algorithm yields multiple distinct networks, but all such LCNs perform roughly equally, all have a "random" appearance, and all outperform our best efforts to directly design a good network. It is also noteworthy that such "evolved" LCNs were found to be insensitive to moderate perturbations to their component values, indicating a high degree of robustness to imperfect implementation.

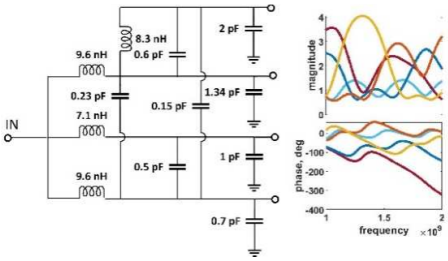

Figure 6. Evolved diversity network optimized for interference suppression

V. EXPERIEMENTAL VALIDATION

We tested the viability of synthetic diversity with an integrated receiver, shown in Fig. 8. The receiver consists of an integrated LC diversity network (Fig. 7) followed by 4 identical receiver channels. Each channel consisted of an inverter-based LNA, followed by a 4-phase passive mixer, driven by 4 shared non-overlapping quadrature LO signals derived from a frequency divide-by-2. After down conversion, each receiver contains two stages of baseband low-pass filtering with 10 MHz cut off frequency, and amplification, with the second stage performing differential-to-single-ended conversion to save bond pads.

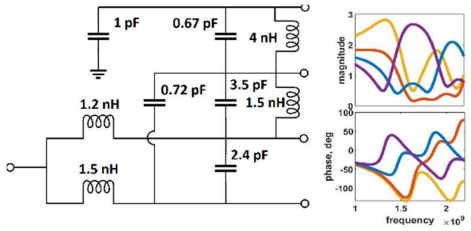

Figure 7. Implemented LCN schematic and transfer functions

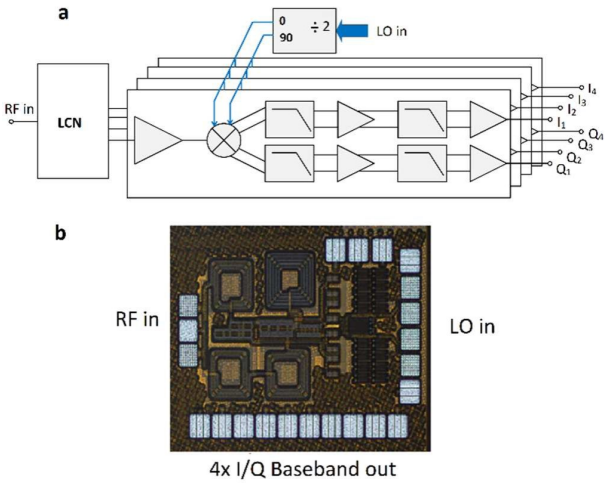

Figure 8: block diagram and die photo. Die dimensions: 1mm x 0.7mm.

A. Chip Characterization

To characterize the diversity provided by the LCN, QPSK-modulated signal was applied to the input at different frequencies. Fig. 9 (a) shows the absolute value of the strongest PC component for the four output channels, i.e. normalized gain of each channel since there was only one strong PC. Fig. 9 (b) shows the phase of the strongest PC component for different channels relative to ch1. The gains and relative phase of the four channels vary noticeably over frequency which is desired.

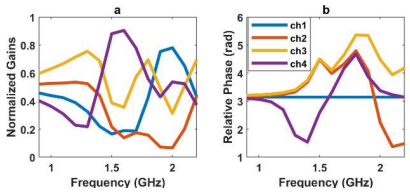

Figure 9. Measurement results for normalized gain of the four different channels and relative phase of the channels to channel 1.

Fig. 10 (a) shows the measurement results of noise figure (NF) over frequency. Minimum NF is 4.03dB at 1.1GHz while the highest NF reaches 10.2dB at 1.7GHz. Fig. 10 (b) shows P-1db due to Interferer, where the signal power is -73.4dBm while the power of the interferer at 100MHz offset from signal is increased to the point at which the signal output power gets attenuated by 1dB. This is an important metric for our measurements, since we want to make the interferer large enough to generate considerable in-band artifacts while staying away from compression point.

Less than 10.2dB NF and higher than -18.9dBm P-1dB due to interferer allow us to apply interferer levels as high as

70dB larger than the signal level and still stay away from both the compression point and the noise floor.

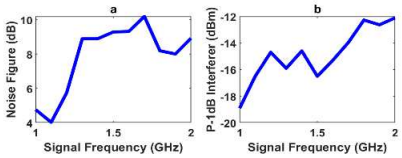

Figure 10. Measurement results of NF and P-1db due to interferer vs F_{Sig}

B. Interference suppression

To calculate signal CGVs, we first applied 1MSPS QPSK-modulated Manchester-coded signals at different frequencies and performed PCA on the recorded data. Two methods were used to find artifact CGVs: 1) Only the interferer was applied as input ("Int-only") at different frequencies and the CGVs were calculated by performing PCA, 2) A blind algorithm proposed in [7] ("Algorithm") was used to find the interferer CGVs using the data when both signal and interferer are present. These signal and interferer CGVs were then used to suppress artifacts when both signal and interference were present as explained in section III.

1) Suppression of Spur-induced Artifacts

A -41dBc spur at 400MHz offset from the carrier frequency was added to the LO A single tone interferer at 400.9MHz offset from the signal was also applied. An example of the measurements is shown in Fig. 11. Note that ch1 is completely dominated by the 900kHz IBA, while other channels show a mixture of QPSK and sine wave constellations. Corrected versions; however, are much cleaner with zero BER and lower EVM. Fig. 12 presents EVM and BER over frequency. For all frequencies, the corrected BERs (black and blue lines) are lower than the channel with the best BER at that frequency, what a bank of selectable band-pass filters (BBPFs) could provide. The EVM is also improved for all cases except for 1.4GHz for Algorithm.

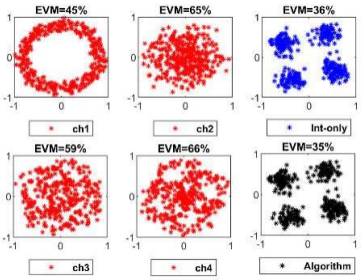

Figure 11. Sample constellations for spur measurements before Manchester decoding. Signal is -86.4dBm at 1.6GHz and interferer is -26dBm at 2GHz.

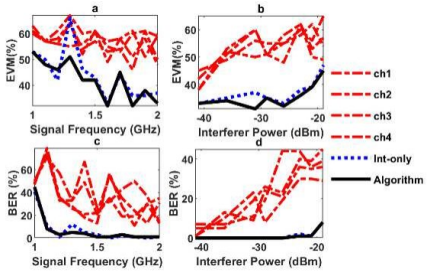

Figure 12. Measurement results for spur artifacts. Signal power is -86.4dBm. a and c: interferer power is -26dBm. b and d: F_{Sig}=1.6GHz and F_{Int}=2GHz.

We also swept interfere power and measured EVM and BER as shown in Fig. 10 (b), (d). As the interferer power increases, the improvement in BER gained by using SD becomes more significant (BER is less than 2% for interferers as large as -21dBm); however, it fails if the interferer is large enough, for this case -19dBm.

2) Suppression of Phase noise-induced Artifacts

Phase noise was added to the LO by first attenuating the LO by 71dB and then re-amplifying it back. An interferer was generated at 100MHz offset from the signal. Fig. 13 shows example constellations: though phase-noise reciprocal mixing completely buries the signal in each channel SD allowed the signal to be recovered with zero BER. Fig. 14 (a), (c) show performance over frequency. BER for the corrected data is again lower than the best BER channel for all cases. For 1GHz signal, improvement is negligible due to lack of diversity between signal and interferer. Fig. 14 (b), (d) show that the SD successfully suppresses artifacts from interferers as large as -21 dBm with less than 2% BER.

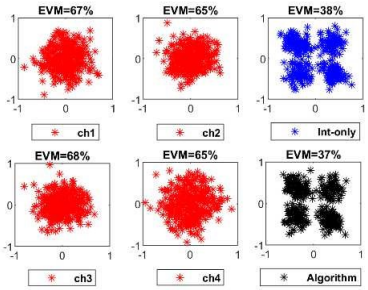

Figure 13. Sample constellations for spur measurements before Manchester decoding. Signal is -83.4dBm at 1.6GHz and interferer is -26dBm at 1.7GHz.

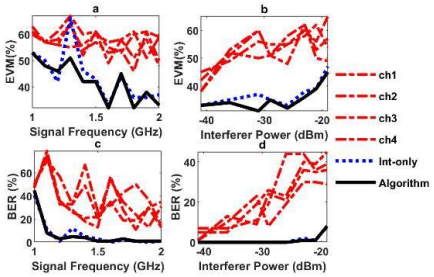

Figure 14. Measurement results for PN artifacts. Signal power is -83.4dBm. a and c: interferer power is -26dBm. b and d: F_{Sig}=1.6GHz and F_{Int}=1.7GHz.

VI. CONCLUSION

Deliberate introduction of diversity in phase and gain, as a function of frequency, was shown to provide sufficient information to separate a desired, in band signal from in-band artifacts generated by an out-of-band interferer. This method worked for suppressing phase noise and spur effects. Critically, the required weights for interference suppression could be achieved using a blind algorithm, which does not require prior knowledge of the interferer's frequency or transfer functions.

Overall, this work demonstrates, experimentally, that Synthetic diversity provides a new, robust path to increasing interference tolerance in widely tunable RF receivers.

ACKNOWLEDGMENT

The authors would like to thank BP Paris's and A El-Ghazaly's invaluable comments and advices.

REFERENCES

[1] L. van der Perre et al., "Architectures and Circuits for Software-Defined Radios: Scaling and Scalability for Low Cost and Low Energy," 2007 IEEE International Solid-State Circuits Conference. Digest of Technical Papers, San Francisco, CA, 2007, pp. 568-569, doi: 10.1109/ISSCC.2007.373547.

[2] J. Craninckx et al., "A Fully Reconfigurable Software-Defined Radio Transceiver in 0.13µm CMOS," 2007 IEEE International Solid-State Circuits Conference. Digest of Technical Papers, San Francisco, CA, 2007, pp. 346-607, doi: 10.1109/ISSCC.2007.373436.

[3] J. Borremans, et al., "A 40 nm CMOS 0.4–6 GHz Receiver Resilient to Out-of-Band Blockers," in IEEE Journal of Solid-State Circuits, vol. 46, no. 7, pp. 1659-1671, July 2011, doi: 10.1109/JSSC.2011.2144110.J.

[4] Y. Lien, E. Klumperink, B. Tenbroek, J. Strange and B. Nauta, "A mixer-first receiver with enhanced selectivity by capacitive positive feedback achieving +39dBm IIP3 and <3dB noise figure for SAW-less LTE Radio," 2017 IEEE Radio Frequency Integrated Circuits Symposium (RFIC), Honolulu, HI, 2017, pp. 280-283, doi: 10.1109/RFIC.2017.7969072.

[5] E. C. Szoka and A. Molnar, "Circuit Techniques for Enhanced Channel Selectivity in Passive Mixer-First Receivers," 2018 IEEE Radio Frequency Integrated Circuits Symposium (RFIC), Philadelphia, PA, 2018, pp. 292-295, doi: 10.1109/RFIC.2018.8429040.

[6] C. Andrews and A. C. Molnar, "A Passive Mixer-First Receiver With Digitally Controlled and Widely Tunable RF Interface," in IEEE Journal of Solid-State Circuits, vol. 45, no. 12, pp. 2696-2708, Dec. 2010, doi: 10.1109/JSSC.2010.2077151.

[7] A. Molnar, Z. Boynton, S. Soni and S. Sadeghi, "Synthetic Diversity To Mitigate Out-of-Band Interference in Widely Tunable Wireless Receivers," 2019 53rd Asilomar Conference on Signals, Systems, and Computers, Pacific Grove, CA, USA, 2019, pp. 774-778, doi: 10.1109/IEEECONF44664.2019.90486

[8] T. Tapen, Z. Boynton, H. Yüksel, A. Apsel and A. Molnar, "The Impact of LO Phase Noise in N-Path Filters," in IEEE Transactions on Circuits and Systems I: Regular Papers, vol. 65, no. 5, pp. 1481-1494, May 2018, doi: 10.1109/TCSI.2017.2761260.